Graefe's Archive for Clinical and Experimental Ophthalmology (2022) 260:1525–1534
https://doi.org/10.1007/s00417-021-05337-3

RETINAL DISORDERS

Choroidal vascularity index in eyes with central macular atrophy secondary to age-related macular degeneration and Stargardt disease

Eleonora Corbelli[1,2] · Riccardo Sacconi[1,2] · Marco Battista[1,2] · Daniela Bacherini[3] · Alexandra Miere[4] · Enrico Borrelli[1,2] · Eliana Costanzo[5] · Giovanna Vella[2,6] · Mariacristina Parravano[5] · Lucia Ziccardi[5] · Andrea Sodi[3] · Stanislao Rizzo[7,8,9] · Eric H Souied[4] · Francesco Bandello[1,2] · Giuseppe Querques[1,2]

Received: 22 February 2021 / Revised: 7 July 2021 / Accepted: 22 July 2021 / Published online: 20 January 2022

Abstract

Purpose To compare macular atrophy (MA) secondary to age-related macular degeneration (AMD) and Stargardt disease (STGD) using the choroidal vascularity index (CVI).

Methods In this multicentric retrospective study, two distinct cohorts were collected: patients with MA secondary to AMD and MA secondary to STGD. All patients were investigated using a multimodal imaging approach, including CVI in the subfoveal 1000 μm area. Of note, the CVI is not influenced by aging, which allows comparisons between different cohorts.

Results Seventy eyes were included: 35 eyes of 35 patients (mean age 78 ± 7 years) in the AMD group and 35 eyes of 35 patients (mean age 41 ± 16 years, $p < 0.001$) in the STGD group. Choroidal thickness was significantly lower in the AMD group in comparison to the STGD group (151 ± 80 μm vs 353 ± 105 μm, $p < 0.001$). The total choroidal area (TCA) was significantly greater in the STGD group in comparison to the AMD group (1.734 ± 0.958 mm^2 vs 0.538 ± 0.391 mm^2, respectively, $p < 0.001$).

Interestingly, the CVI was significantly lower in AMD patients in comparison to STGD patients (27.322 ± 15.320% vs 49.880 ± 7.217%, respectively, $p < 0.001$), and this difference was confirmed in the subgroup of patients over 50 years old.

Conclusion Our results corroborate the hypothesis that large choroidal vessels were impaired to a greater extent in AMD than in STGD. CVI may help in differentiating AMD from STGD in the presence of MA, better understanding of the pathogenesis, and monitoring of therapeutic response.

Keywords Age-related macular degeneration · Choroidal vascularity index · Geographic atrophy · Macular atrophy · Stargardt disease

Eleonora Corbelli and Riccardo Sacconi contributed equally to this work.

✉ Giuseppe Querques
giuseppe.querques@hotmail.it; querques.giuseppe@hsr.it

[1] School of Medicine, Vita-Salute San Raffaele University, Milan, Italy

[2] Division of head and neck, Ophthalmology Unit, IRCCS San Raffaele Scientific Institute, Milan, Italy

[3] Department of Neurosciences, Psychology, Drug Research and Child Health Eye Clinic, University of Florence, AOU Careggi, Florence, Italy

[4] Department of Ophthalmology, Hospital Intercommunal de Creteil, University Paris Est Creteil, Creteil, France

[5] Foundation G.B. Bietti-IRCCS, Rome, Italy

[6] Ophthalmology, Department of Surgical, Medical, Molecular Pathology and of Critical Area, University of Pisa, Pisa, Italy

[7] UOC Oculistica, Fondazione Policlinico Universitario A. Gemelli IRCCS, Rome, Italy

[8] Università Cattolica del Sacro Cuore, Rome, Italy

[9] Consiglio Nazionale delle Ricerche, Istituto di Neuroscienze, Pisa, Italy

Key messages

What was known

- Macular atrophy represents the common late-stage manifestation of various retinal diseases including age-related macular degeneration (AMD) and Stargardt disease (STGD)
- Distinguishing macular atrophy secondary to dry AMD from atrophy of retinal pigment epithelium associated with the late form of STGD could be challenging

That this paper adds

- A major and clinically significant choroidal vascularity index (CVI) reduction was found in eyes with MA secondary to AMD as compared with MA associated with STGD
- CVI could be a useful tool for correct diagnosis, better understanding of the pathogenesis of these disorders, and potential monitoring of therapeutic response including new therapeutic strategies

Introduction

Macular atrophy (MA) is defined as the presence of areas of retinal pigment epithelium (RPE) atrophy with increased signal transmission through the choroid and collapse or thinning of the outer retinal layer [1]. Such MA represents the common late-stage manifestation of various retinal diseases, including age-related macular degeneration (AMD) [i.e., geographic atrophy (GA)] and Stargardt disease (STGD).

Geographic atrophy secondary to dry AMD affects up to 22% of people aged over 90 years and multiple pathophysiological mechanisms are hypothesized to be behind the disease [2]. Oxidative damage, vascular insufficiency, and inflammation are considered responsible for RPE, photoreceptor, and choriocapillaris (CC) injury [3–7]. Stargardt disease, one of the most common inherited retinal dystrophies, causes central vision loss in childhood or early adulthood according to a well-known process. Mutations in the ABCA4 gene result in the increased production and accumulation in the RPE of a lipofuscin fluorophore named N-retinylidene-N-retinylethanolamine (A2E) causing loss of RPE cells and formation of MA [8–10].

It could be very challenging to differentiate MA secondary to AMD and to STGD, especially in the absence of pathognomic hallmarks such as drusen and flecks, respectively. Macular atrophy secondary to AMD and STGD appears ophthalmoscopically as a unifocal or multifocal area of partial or complete depigmentation in the macular region with visible underlying choroidal vessels, while on fundus autofluorescence (FAF) both look as distinct dark spaces due to the absence of lipofuscin-containing cells [11].

Fluorescein angiography (FA) and indocyanine green angiography (ICGA) are useful tools for a diagnostic and pathogenetic distinction of the two diseases. In STGD, FA shows the dark choroid, a typical sign due to absorption of the blue excitatory light by lipofuscin, resulting in the absence of normal background fluorescence [12]. Moreover, even in patients affected by STGD with no evidence of dark choroid on FA images, ICGA could be able to reveal hypocyanescence within the area of MA [13]. This ICGA sign could be correlated to CC damage, as supported by extensive loss of CC in the analysis of MA by optical coherence tomography angiography (OCT-A) in patients with STGD [14].

Taking this into consideration, in our paper, we investigated MA secondary to AMD and STGD using a new imaging tool, the choroidal vascularity index (CVI), for the measurement and analysis of the choroidal vasculature system by quantifying both luminal and stromal choroidal components. Of note, we use the CVI parameter in our analysis because CVI is less influenced by aging in comparison to choroidal thickness, although the influence of aging remains debated [15, 20]. The aim of this study is to evaluate a possible role of CVI for differential diagnosis and, more importantly, to investigate additional differences in the pathogenesis of MA secondary to AMD and STGD.

Methods

In this retrospective cohort study, participants were collected from four retina referral centers (the Medical Retina & Imaging Unit of the Department of Ophthalmology of University Vita-Salute San Raffaele in Milan, Italy; the Department of Ophthalmology of University Paris Est, in Creteil, France; the Department of Ophthalmology of IRCCS-Fondazione Bietti in Rome, Italy; the Department of Ophthalmology of Eye Clinic, University of Florence, AOU Careggi, Florence, Italy) evaluated between January 2019 and

December 2019. The study was conducted in agreement with the Declaration of Helsinki for research involving human participants and was approved by the Ethics Committee for all sites.

The present study consists of the following two distinct cohorts: patients with MA secondary to AMD and secondary to STGD.

Inclusion criteria for both cohorts were: (1) at least one well-defined area of apparent absence of the RPE with or without foveal involvement and with a minimal extent of 0.05 mm^2 (the size of the smallest atrophic area in cases of multifocality); (2) clear ocular media to ensure proper image quality. Absence of RPE was disclosed using FAF as the area with hypoautofluorescence.

For inclusion into the AMD group, age over 50 years and drusen and/or retinal pigment abnormalities consistent with the diagnosis of AMD had to be present in the eye with GA and/or in the fellow eye.

Diagnostic criteria for STGD included decreased visual acuity (VA) due to macular dystrophy associated with multiple fundus flecks. Patients affected by STGD were classified in three different clinical phenotypes according to the classification of Fishman et al. [21]. Briefly, phenotype 1 is characterized by small, atrophic-appearing foveal lesion surrounded by parafoveal or perifoveal yellowish white lesions; phenotype 2 is characterized by yellowish white fundus lesions occurred throughout the posterior pole; phenotype 3 is characterized by extensive atrophic-appearing changes of the RPE throughout the posterior pole extending beyond the vascular arcades.

If both eyes presented inclusion criteria, only one was included. The eye with the higher quality of OCT images was selected as the study eye. If both eyes of the same patient have the same quality of OCT images, the included eye was randomly selected by flipping a coin.

The exclusion criteria were: (1) any other cause of chorioretinal atrophy (e.g., myopia, pattern dystrophies, central areolar macular atrophy, retinitis pigmentosa, rod-cone dystrophies, Best disease, Sorsby macular dystrophy, chorioretinal inflammatory diseases, drug-induced retinopathy, post-traumatic atrophy); (2) presence of any retinal disorder potentially confounding the clinical assessment (e.g., diabetic retinopathy, retinal vein occlusion, retinal artery occlusion); (3) signs of macular neovascularization (MNV), including intraretinal or subretinal fluid, hemorrhage, subretinal fibrosis; (4) any previous treatment (e.g., laser photocoagulation, photodynamic therapy, intravitreal injections of antivascular endothelial growth factors or steroids); (5) myopia greater than 6 diopters (D) of sphere or 3 D of cylinder, and/or axial length greater than 25.5 mm.

As part of standard clinical assessment, all participants underwent a complete ophthalmologic examination, including Snellen best-corrected VA (BCVA) that was converted to the logarithm of the minimum angle of resolution (LogMAR) for statistical analysis, slit-lamp biomicroscopy, and indirect fundus ophthalmoscopy. Furthermore, all patients underwent multimodal imaging evaluation, including infrared reflectance (IR), FAF, and structural spectral domain optical coherence tomography (SD-OCT) that were performed using the Spectralis HRA + OCT system (Heidelberg Engineering, Heidelberg, Germany). To achieve good visualization of the choroid, enhanced depth imaging (EDI) OCT was used in all acquisitions. FA was also recorded when available. FA was performed using the Spectralis HRA + OCT (Heidelberg Engineering, Heidelberg, Germany) or TRC-501X (Topcon, Inc., Tokyo, Japan) machines.

Axial length was measured using a noncontact biometry instrument (IOLMaster [Carl Zeiss Meditec AG, Jena, Germany]). When available, ABCA4 genotyping of STGD patients was recorded and reported.

Clinical findings and multimodal imaging features were collected and analyzed.

Central macular thickness (CMT) was assessed in the central 1-mm-diameter circle of ETDRS thickness map using Spectralis software (Heidelberg Eye Explorer 1.9.11.0, Heidelberg, Germany). In each patient, the center of the ETDRS thickness map and the automatic segmentations were checked and manually adjusted in case of error by the Spectralis software.

The RPE atrophic area was manually measured by two independent and experienced readers (MB and EB) as the sum of the hypoautofluorescent areas using FAF images and expressed in mm^2. Choroidal thickness (ChT) was manually measured by two independent and experienced readers (MB and EB) as the distance between the Bruch's membrane interface and the sclerochoroidal interface under the fovea, and at 500 μm nasally and temporally to the fovea. The mean values were considered for statistical analysis.

In order to obtain the CVI, structural OCT passing through the fovea was analyzed and processed using the software FIJI (National Institute of Health, Bethesda, MD, USA) with a previously published method [22, 23]. In detail, horizontal structural OCT passing thought the fovea was acquired using Spectralis with a scan angle of 30°, ART mode on with 50 images averaged, and EDI mode on, as for our clinical practice. The quality of the images was checked by an expert grader (R.S.). In case of low-quality images, or not centered images, the patient was not included in the analysis. The OCT image was imported in the FIJI software, and the subfoveal 1000 μm region centered on the fovea was selected as the region of interest (ROI) using the polygon tool, as previously reported [24]. The upper and the lower boundaries of the ROI was selected as the choroidal-RPE junction and the sclerochoroidal junction. In case of RPE absence, the choroidal-RPE junction was selected at the level of the Bruch's membrane. After that, the image was binarized using

the Niblack's autolocal threshold. The total choroidal area (TCA) was defined as the total area of the ROI. The luminal choroidal area (LCA) was represented by the black pixels and stromal choroidal area (SCA) by the white pixels. The TCA, LCA, and SCA are measured. The CVI was calculated as the ratio between LCA and TCA.

Statistical analysis

Statistical analyses were performed using SPSS Statistics Version 20 (IBM, Armonk, New York, USA). All values of descriptive analyses were reported as counts (percentages) for categorical variables, and as means±standard deviation for continuous variables. The agreement between individual measurements of RPE atrophic areas and ChT from both readers was performed using the intraclass correlation coefficient (ICC; 95% CI). Comparisons of BCVA, RPE atrophic area, axial length, CMT, ChT, TCA, LCA, SCA, and CVI between the two groups were performed using the independent samples Student t-test. The analyses of CVI, TCA, LCA, and SCA among the different phenotypes of STGD were performed using the analysis of variance (ANOVA) with Bonferroni post-hoc analysis. The correlations between RPE atrophic area with CVI, TCA, LCA, and SCA were investigated using the Pearson correlation coefficient. In all analyses, p-values <0.05 were considered as statistically significant.

Results

Seventy eyes of 70 Caucasian patients fulfilled the inclusion and exclusion criteria and were included in the study. Thirty-five eyes of 35 patients (mean age 78 ± 7 years, median 78; range 68–94 years) were included in the AMD group and 35 eyes of 35 patients (mean age 41 ± 16 years, median 42; range 20–78 years; $p < 0.001$) were included in the STGD group. ABCA4 mutations were available for 20 out of 35 patients (Table E1).

The two groups did not show statistical differences in terms of BCVA, RPE atrophic area, and axial length ($p = 0.205$, $p = 0.122$, and $p = 0.515$, respectively), whereas CMT was significantly lower in patients affected by Stargardt disease ($p < 0.001$) (Table 1). Considering the STGD group, 8 eyes were classified as phenotype 1, 8 eyes as phenotype 2, and 19 eyes as phenotype 3.

Furthermore, we analyzed the subgroup of patients over 50 years old in the STGD group (12 eyes of 12 patients, mean age 60 ± 10 years, median 57, range 50–78 years) compared with overall AMD cases. Also in this sub-analysis, the two groups did not show statistical differences in terms of BCVA, RPE atrophic area, and axial length ($p = 0.277$, $p = 0.229$, and $p = 0.915$, respectively), whereas CMT was significantly lower in patients affected by Stargardt disease ($p < 0.001$) (Table E2). However, GA patients showed a significantly greater age in comparison with this STGD subgroup ($p < 0.001$) (Table E2).

Choroidal analysis

Comparing ChT between AMD and STGD patients, the latter showed a significantly thicker ChT with respect to subfoveal, nasal, and temporal locations (Table 1). In detail, subfoveal ChT was 151 ± 80 μm (median, 127; range 45–399 μm) and 353 ± 105 μm (median, 355; range 80–619 μm) ($p < 0.001$) in AMD and SGTD groupS, respectively, and the same trend was disclosed in 500 μm nasally and temporally to the fovea ($p < 0.001$ in both analyses) (Table 1). Interobserver variability between readers was excellent for all measurements [ICC = 0.953 (0.925–0.981)]. Following the ChT trend, the TCA in the 1000 μm centered on the fovea was significantly greater in the STGD group in comparison to the AMD group (1.734 ± 0.958 mm^2 vs 0.538 ± 0.391 mm^2, respectively, $p < 0.001$) (Table 2). This trend was also confirmed in the subanalyses of LCA and SCA (Table 2).

Interestingly, analyzing the ratio between the choroidal LCA and the TCA, the CVI was significantly lower in AMD patients in comparison to STGD patients (27.322 ± 15.320% vs 49.880 ± 7.217%, respectively, $p < 0.001$) (Table 2) (Figs. 1 and 2). In other words, the LCA was impaired to a greater extent in AMD patients in comparison to STGD patients. Furthermore, analyzing the CVI, TCA, LCA, and SCA among the different phenotypes of STGD, we demonstrated that all these parameters are influenced by the stage of the STGD phenotype (ANOVA analysis of CVI, TCA, LCA, and SCA comparing different STGD stages: $p = 0.060$, $p = 0.015$, $p = 0.010$, and $p = 0.033$, respectively (Table 3)). In detail, there was a reduction in values with increasing stages (Table 3).

Interestingly, the same trends were disclosed in the subanalysis of patients over 50 years old in the STGD group in comparison to the AMD group. In detail, the CVI was significantly lower in AMD vs STGD patients (27.322 ± 15.320 vs 45.592 ± 9.670, respectively, $p < 0.001$) (Table 4).

Analyzing the correlation between the RPE atrophic area measured using FAF with CVI, TCA, LCA, and SCA, no significant correlation was disclosed considering all patients ($p > 0.4$ in all analyses using Pearson correlation coefficient), considering only AMD patients ($p > 0.2$ in all analyses using Pearson correlation coefficient), and considering only STGD patients ($p > 0.2$ in all analyses using Pearson correlation coefficient) (Table E3). Furthermore, we have analyzed the correlation between the diameter of the RPE atrophic area of the horizontal b-scan with CVI, TCA, LCA, and SCA. Also in this case, no significant correlations were disclosed ($p > 0.2$ in all analyses using Pearson correlation coefficient).

Table 1 Demographics and main clinical features of the study population

	GA group	STGD group	*P* value
N, eyes (patients)	35 (35)	35 (35)	
Sex, n			
Male	9	14	
Female	26	21	0.203*
Age, years (mean±SD)	78±7	41±16	<0.001§
BCVA, LogMAR (mean±SD)	0.53±0.29	0.63±0.36	0.205§
RPE atrophic area using FAF, mm^2 (mean±SD)	8.14±3.96	6.23±6.02	0.122§
RPE atrophic diameter using OCT, μm (mean±SD)	3234±980	3399±1028	0.498§
Axial length, mm (mean±SD)	23.91±0.44	23.98±0.49	0.515§
CMT, μm (mean±SD)	244±43	116±59	<0.001§
Subfoveal ChT, μm (mean±SD)	151±80	353±105	<0.001§
500 μm nasal ChT, μm (mean±SD)	138±78	332±99	<0.001§
500 μm temporal ChT, μm (mean±SD)	157±77	340±87	<0.001§

GA geographic atrophy, *STGD* Stargardt disease, *N* number, *SD* standard deviation, *BCVA* best-corrected visual acuity, *RPE* retinal pigment epithelium, *FAF* fundus autofluorescence, *OCT* optical coherence tomography, *CMT* central macular thickness; *ChT* choroidal thickness

* Chi-squared test

§ independent samples Student t-test

Discussion

Distinguishing macular atrophy secondary to dry AMD from atrophy of RPE associated with the late form of STGD could be challenging. It has been indeed thoroughly documented that both these retinal diseases develop MA with different mechanisms, even though it remains partially unclear in the case of AMD, and present distinctive progression. [3, 4, 8–10, 25].

Although fundus photography and FAF are useful tools for the detection and follow-up of these diseases [11], they do not give information on the pathogenesis and often do not provide distinctive criteria. Combining multimodal imaging could be a strategy to face this specific, but important, differential diagnosis, in regard to prognosis and design of interventional trials.

Table 2 Choroidal analysis of the GA group vs STGD group

	GA group (n=35)	STGD group (n=35)	*P* value§
LCA, mm^2 (mean±SD)	0.192 ± 0.209	0.912 ± 0.579	<0.001
SCA, mm^2 (mean±SD)	0.347 ± 0.190	0.822 ± 0.389	<0.001
TCA, mm^2 (mean±SD)	0.538 ± 0.391	1.734 ± 0.958	<0.001
CVI (mean±SD)	27.322 ± 15.320	49.880 ± 7.217	<0.001

GA geographic atrophy, *STGD* Stargardt disease, *SD* standard deviation, *LCA* luminal choroidal area, *SCA* stromal choroidal area, *TCA* total choroidal area, *CVI* choroidal vascularity index

§ independent samples Student t-test

Giani et al. [13] conducted a multi-imaging study to characterize RPE atrophy in AMD and STGD with a particular interest in ICGA examination. Confirming previous observations [26], in 92% of eyes affected by STGD, ICGA showed hypofluorescence from the areas of atrophy, more evident in the late phase, defined as dark atrophy [13]. This ICGA finding, identified in only 13% of patients with AMD, has been ascribed to extended damage of CC. This hypothesis has been confirmed by Pellegrini et al. using OCT-A [14]. They described an extensive loss of CC in the central area with persisting tissue at margins of MA secondary to STGD, whereas CC resulted only rarely in patients with MA secondary to AMD [14].

Recently CVI has been proposed as a novel OCT-based parameter to quantify choroidal structural changes in healthy participants [15–20] and in different disorders, including AMD and STGD [27–31]. Giannaccare et al. showed that CVI in patients affected by MA secondary to AMD was progressively reduced during the follow-up period, speculating a possible stromal substitution of the choroidal vessels [32]. Similarly, Ratra et al. [33] found a significant reduction of CVI in STGD versus healthy eyes and a correlation between the reduction of CVI and a deterioration of visual acuity.

However, to our knowledge, in the literature there are no papers comparing CVI in macular atrophy secondary to AMD and STGD. In our study, a major and clinically significant CVI reduction was found in eyes with MA secondary to AMD as compared with MA associated with STGD ($p < 0.001$). This finding could be due to greater impairment of the luminal choroidal area in AMD patients than in STGD

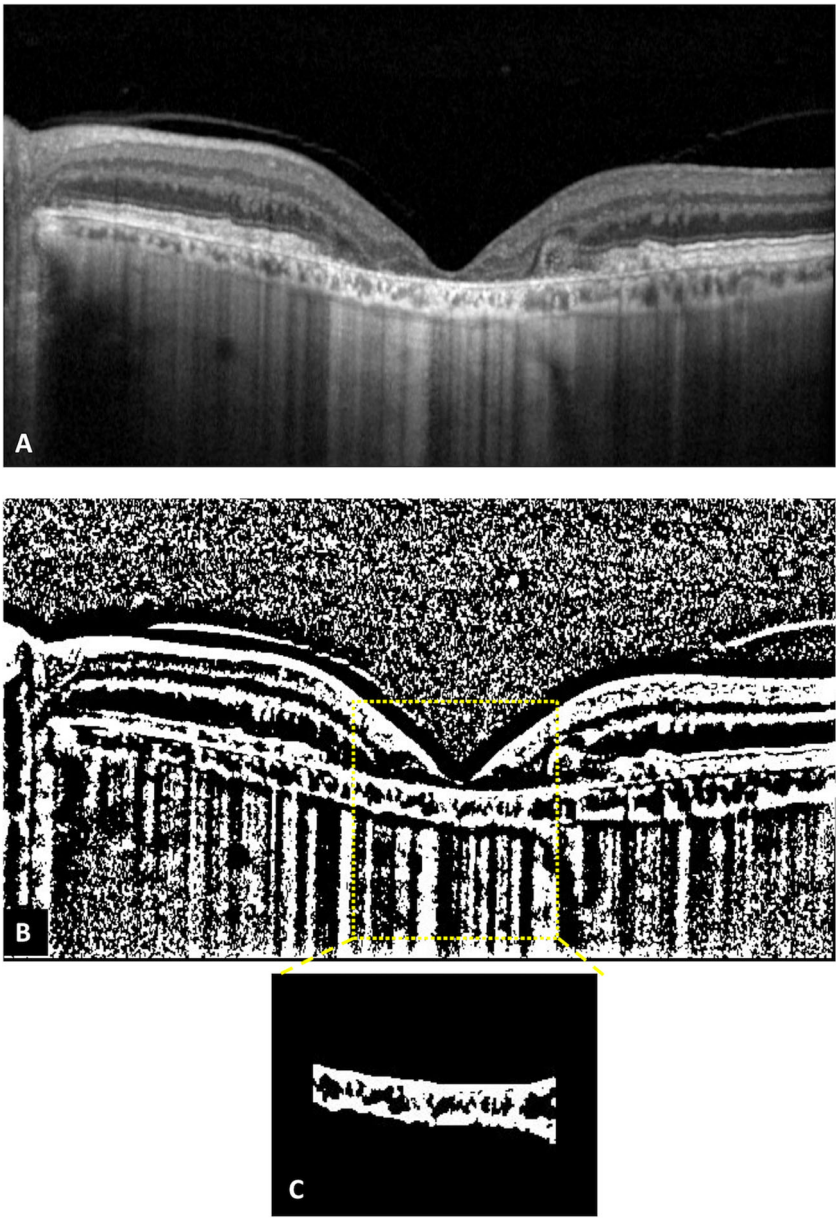

Fig. 1 Structural optical coherence tomography (OCT) and choroidal vascularity index (CVI) calculation of a patient affected by macular atrophy secondary to age-related macular degeneration. Horizontal b-scan structural OCT passing through the fovea showing the presence of retinal pigment epithelium (RPE) atrophy with increased signal transmission through the choroid and collapse or thinning of the outer retinal layer (A). The image was binarized using Niblack's auto-local threshold (B) in order to calculate the CVI. Dark pixels represent the luminal area, whereas white pixels the stromal area. CVI was calculated in the 1000 μm subfoveal area (C) as the ratio between the luminal area and the total choroidal area

patients. Alternatively, this finding may suggest a compensatory dilation of the large choroidal vessels in MA associated with STGD (i.e., higher luminal choroidal area) due to the greater impairment of choriocapillaris in STGD in comparison to AMD. Indeed, in AMD, the partial preservation of CC and the lower vascular reactivity resulting from an increased vascular rigidity (i.e., atherosclerosis) could contribute to a minimal compensatory dilation of choroidal vessels [34].

One may attribute this result to the different average age of the two groups. The influence of aging on CVI remains debated. In a recent study, Zhou et al. [15], using a swept-source OCT, showed that CVI remained constant in all regions with age, while ChT and choroidal volume, even including both choroidal vessels and stroma, decreased with the years. On the other hand, Nivison-Smith et al. [19], using an SD-OCT, showed an age-related decline of CVI with eccentricity. Finally, Kokac et al. [18] reported that CVI was lower in patients under 18 years old in comparison to patients over 18 years old, but this is not the case in our study population. Although the influence of different average age of the two groups cannot be completely excluded, we have analyzed the subfoveal location of the choroid, that is less influenced by aging [15–20]. Furthermore, we found the same trend analyzing only the sub-group of patients over 50 years old affected by STGD in comparison to the AMD group. Particularly, in this age-group >50 years old, CVI could be a

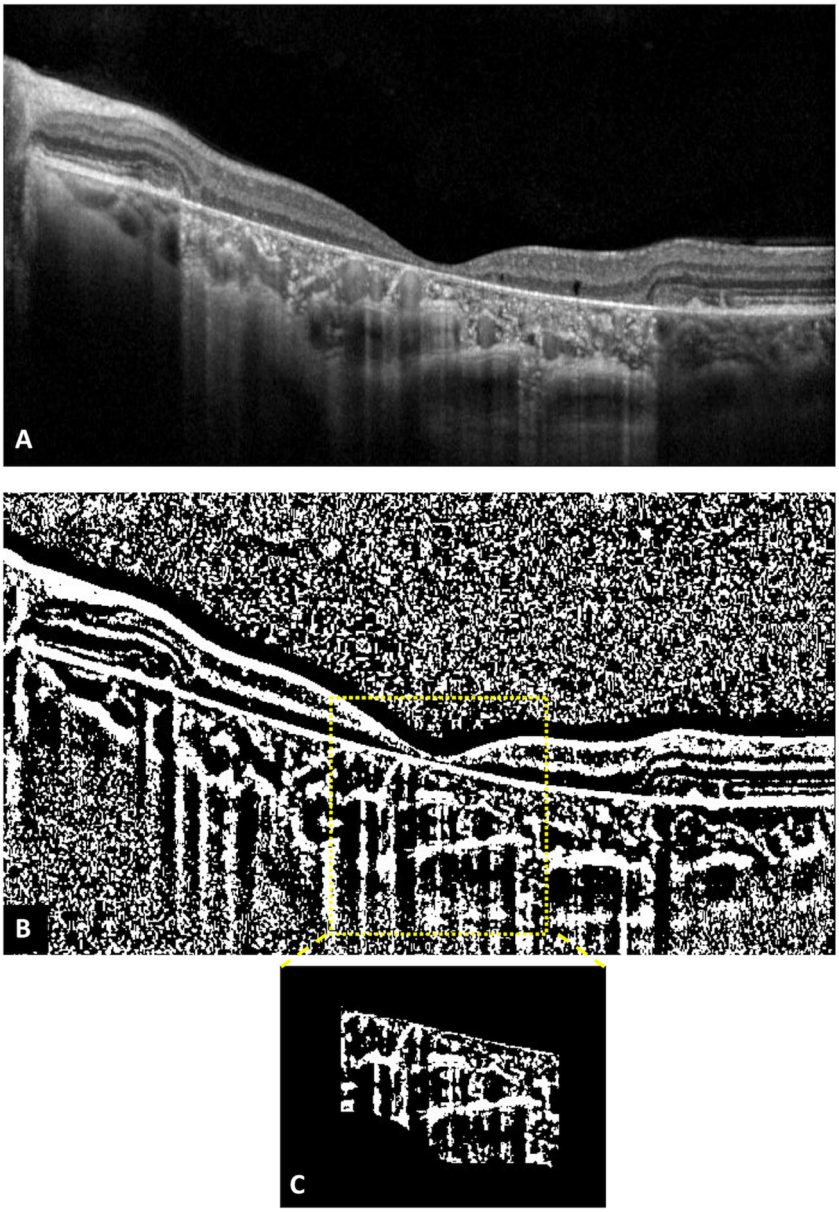

Fig. 2 Structural optical coherence tomography (OCT) and choroidal vascularity index (CVI) calculation of a patient affected by macular atrophy secondary to Stargardt disease. Horizontal b-scan structural OCT passing through the fovea showing the presence of retinal pigment epithelium (RPE) atrophy with increased signal transmission through the choroid and collapse or thinning of the outer retinal layer (A). The image was binarized using Niblack's auto-local threshold (B) in order to calculate the CVI. Dark pixels represent the luminal area, whereas white pixels the stromal area. CVI was calculated in the 1000 μm subfoveal area (C) as the ratio between the luminal area and the total choroidal area

Table 3 Choroidal analysis of the STGD group according to the Fishman stages

	STGD group (n= 35)	Phenotype 1 (*n*= 8)	Phenotype 2 (*n*= 8)	Phenotype 3 (*n*= 19)	*P* value§
LCA, mm^2 (mean± SD)	0.912 ± 0.579	1.415 ± 0.628	0.911 ± 0.542	0.701 ± 0.454	0.010
SCA, mm^2 (mean± SD)	0.822 ± 0.389	1.107 ± 0.460	0.851 ± 0.307	0.689 ± 0.335	0.033
TCA, mm^2 (mean± SD)	1.734 ± 0.958	2.522 ± 1.078	1.761 ± 0.838	1.391 ± 0.780	0.015
CVI (mean±SD)	49.880 ± 7.217	55.077 ± 4.056	48.981 ± 8.586	48.070 ± 6.893	0.060

STGD Stargardt disease, *SD* standard deviation, *LCA* luminal choroidal area, *SCA* stromal choroidal area, *TCA* total choroidal area, *CVI* choroidal vascularity index

§ analysis of variance (ANOVA)

Table 4 Choroidal analysis of the GA group vs STGD subgroup of patients over 50 years old

	GA group (n=35)	STGD group (*n*=12)	*P* value§
LCA, mm^2 (mean±SD)	0.192 ± 0.209	0.756 ± 0.554	<0.001
SCA, mm^2 (mean±SD)	0.347 ± 0.190	0.751 ± 0.341	<0.001
TCA, mm^2 (mean±SD)	0.538 ± 0.391	1.507 ± 0.888	<0.001
CVI (mean±SD)	27.322 ± 15.320	45.592 ± 9.670	<0.001

GA geographic atrophy, *STGD* Stargardt disease, *SD* standard deviation, *LCA* luminal choroidal area, *SCA* stromal choroidal area, *TCA* total choroidal area, *CVI* choroidal vascularity index

§ independent samples Student t-test

clinically key role for a correct differential diagnosis, considering that it is challenging to make the proper diagnosis in older people with MA in absence of specific hallmarks.

Based on our results, we hypothesize that the lower CVI here found in AMD patients in comparison to STGD patients is possibly due to the different pathogenic disease mechanisms rather than different age. Furthermore, these data support the concept that choroidal vascular degeneration could contribute to MA in AMD etiopathogenesis and progression. Indeed, Giannaccare et al. [32] reported that CVI is reduced in patients affected by GA, and that this parameter worsened during the follow-up period.

Furthermore, although we cannot directly compare the CVI of healthy patients reported in previous studies with GA and STGD patients of the current study due to different methodology of the studies, our results suggested that CVI is lower in GA and STGD patients (mean CVI of 27.322% and 49.880%, respectively) in comparison to healthy participants (mean reported CVI between 46% and 70%). These results confirm the data previously reported by Ratra et al. [33] and Giannaccare et al. [32] showing lower CVI in STGD and GA patients, respectively.

Our results support the role of CVI in gathering insights about the pathophysiology of the two distinct diseases and its potential clinical application in the differential diagnosis of patients with MA, especially in STGD cases characterized by a late-onset atrophy development that may be misdiagnosed as AMD. In addition, these outcomes find agreement with the available literature, which supports the advantage of CVI as a more sensitive biomarker in detecting choroidal changes as compared to subfoveal ChT. Indeed, ChT is influenced by the age of patients, and this could be a greater confounding factor in the analysis of results. We found a significantly lower ChT in AMD patients than in STGD patients. This result is in agreement with a previous study reporting a statistically significant increase in the ChT of STGD eyes compared with AMD eyes [35]. However, we cannot exclude that this difference in our series was due to the different mean age of our groups. Another limitation of the ChT analysis is that it does not give structural information. On the other hand, choroidal vascularity index, encompassing changes in both the vascular and stromal component of the choroid, revealed interesting considerations.

Several limitations of our study should be disclosed. First, the relatively small sample of patients included. However, it should be considered that macular atrophy secondary to STGD is a relatively infrequent manifestation. Moreover, although GA was present in both eyes of a patient, we included only one eye in the attempt to reduce any selection bias. Second, the wide age disparity between patients with AMD and STGD. However, it was previously demonstrated that age does not influence the CVI, remaining constant with ageing [15], although the influence of aging remains debated [16–20]. Another limitation of our study was the possible influence of backscattering and shadowing effects due to the RPE absence patients affected by GA and STGD. However, in order to minimize this possible influence, we have used a compensated method of binarization based on two different strategies: first the brightness of the image was adjusted using the average value obtained from the lumen of three major choroidal vessels of the ROI; second, we used an autolocal threshold (Niblack's autolocal threshold) [22, 23].

Finally, the lack of genetic confirmation for all patients affected by STGD and the absence of information on AMD group genotype. Although we did not have genetic mutations for all patients affected by STGD, we included only participants with unequivocal diagnosis due to the presence of flecks in one or both eyes.

Despite these limitations, we believe this study shows a possible role of this novel OCT parameter named CVI as a useful tool for correct diagnosis and better understanding of the pathogenesis of these disorders.

Supplementary Information The online version contains supplementary material available at https://doi.org/10.1007/s00417-021-05337-3.

Declarations

Potential conflicts The authors have no proprietary/financial interest regarding the publication of this study.

Eleonora Corbelli, Marco Battista, Daniela Bacherini, Alexandra Miere, Eliana Costanzo, Giovanna Vella, Lucia Ziccardi, Andrea Sodi and Stanislao Rizzo have nothing to disclose.

Riccardo Sacconi reports personal fees from Novartis (Basel, Switzerland), Zeiss (Dublin, USA) outside the submitted work.

Enrico Borrelli reports personal fees from Novartis (Basel, Switzerland), Zeiss (Dublin, USA) outside the submitted work.

Mariacristina Parravano reports personal fees from Allergan Inc. (Irvine, California,USA), Bayer Shering-Pharma (Berlin, Germany), Novartis (Basel, Switzerland), Zeiss (Dublin, USA) outside the submitted work.

Eric Souied reports personal fees from Allergan Inc. (Irvine, California,USA), Bayer Shering-Pharma (Berlin, Germany), Novartis

(Basel, Switzerland), Roche (Basel, Switzerland) outside the submitted work.

Francesco Bandello reports personal fees from Alcon (Fort Worth,Texas,USA), Alimera Sciences (Alpharetta, Georgia, USA), Allergan Inc. (Irvine, California,USA), Farmila-Thea (Clermont-Ferrand, France), Bayer Shering-Pharma (Berlin, Germany), Bausch And Lomb (Rochester, New York, USA), Genentech (San Francisco, California, USA), Hoffmann-La-Roche (Basel, Switzerland), NovagaliPharma (Évry, France), Novartis (Basel, Switzerland), Sanofi-Aventis (Paris, France), Thrombogenics (Heverlee,Belgium), Zeiss (Dublin, USA) outside the submitted work.

Giuseppe Querques reports personal fees from Alimera Sciences (Alpharetta, Georgia, USA), Allergan Inc. (Irvine, California,USA), Amgen (Thousand Oaks, USA), Heidelberg (Germany), KBH (Chengdu, China), LEH Pharma (London, UK), Lumithera (Poulsbo, USA), Novartis (Basel, Switzerland), Bayer Shering-Pharma (Berlin, Germany), Sandoz (Berlin, Germany), Sifi (Catania, Italy), Soof-Fidia (Albano, Italy), Zeiss (Dublin, USA) outside the submitted work.

Ethical approval All procedures performed in studies involving human participants were in accordance with the ethical standards of the San Raffaelle Ethics Committee and with the 1964 Helsinki declaration and its later amendments or comparable ethical standards.

Informed consent Informed consent was obtained from all individual participants included in the study.

References

1. Gune S, Abdelfattah NS, Karamat A et al (2020) Spectral-domain OCT-based prevalence and progression of macular atrophy in the HARBOR study for Neovascular age-related macular degeneration. Ophthalmology 127:523–532
2. Sacconi R, Corbelli E, Querques L et al (2017) A review of current and future management of geographic atrophy. Ophthalmol Ther 6: 69–77
3. Bhutto I, Lutty G (2012) Understanding age-related macular degeneration (AMD): relationships between the photoreceptor/retinal pigment epithelium/Bruch's membrane/choriocapillaris complex. Mol Asp Med 33:295–317
4. Querques G, Bandello F, Sacconi R et al (2017) Recent advances in the management of dry age-related macular degeneration: a review. F1000Res 6:245
5. Sacconi R, Corbelli E, Borrelli E et al (2021) Choriocapillaris flow impairment could predict the enlargement of geographic atrophy lesion. Br J Ophthalmol 105:97–102
6. Sacconi R, Corbelli E, Carnevali A et al (2018) Optical coherence tomography angiography in geographic atrophy. Retina 38:2350–2355
7. Corbelli E, Sacconi R, Rabiolo A et al (2017) Optical coherence tomography angiography in the evaluation of geographic atrophy area extension. Invest Ophthalmol Vis Sci 58:5201–5208
8. Cideciyan AV, Aleman TS, Swider M et al (2004) Mutations in ABCA4 result in accumulation of lipofuscin before slowing of the retinoid cycle: a reappraisal of the human disease sequence. Hum Mol Genet 13:525–534
9. Mata NL, Weng J, Travis GH (2000) Biosynthesis of a major lipofuscin fluorophore in mice and humans with ABCR-mediated retinal and macular degeneration. Proc Natl Acad Sci U S A 97: 7154–7159
10. Klevering BJ, Deutman AF, Maugeri A et al (2005) The spectrum of retinal phenotypes caused by mutations in the ABCA4 gene. Graefes Arch Clin Exp Ophthalmol 243:90–100
11. Wang DL, Agee J, Mazzola M et al (2019) Outer retinal thickness and fundus autofluorescence in geographic atrophy. Ophthalmol Retin 3:1035–1044
12. Fish G, Grey R, Sehmi KS, Bird AC (1981) The dark choroid in posterior retinal dystrophies. Br J Ophthalmol 65:359–363
13. Giani A, Pellegrini M, Carini E et al (2012) The dark atrophy with indocyanine green angiography in stargardt disease. Investig Ophthalmol Vis Sci 53:3999–4004
14. Pellegrini M, Acquistapace A, Oldani M et al (2016) Dark atrophy: an optical coherence tomography angiography study. Ophthalmology 123:1879–1886
15. Zhou H, Dai Y, Shi Y et al (2020) Age-related changes in choroidal thickness and the volume of vessels and stroma using swept-source OCT and fully automated algorithms. Ophthalmol Retin 4:204–215
16. Agrawal R, Gupta P, Tan KA, Cheung CM, Wong TY, Cheng CY (2016) Choroidal vascularity index as a measure of vascular status of the choroid: measurements in healthy eyes from a population-based study. Sci Rep 6:21090
17. Goud A, Singh SR, Sahoo NK et al (2019) New insights on choroidal vascularity: a comprehensive topographic approach. Invest Ophthalmol Vis Sci 60:3563–3569
18. Koçak N, Subaşı M, Yeter V (2021) Effects of age and binarising area on choroidal vascularity index in healthy eyes: an optical coherence tomography study. Int Ophthalmol 41:825–834
19. Nivison-Smith L, Khandelwal N, Tong J, Mahajan S, Kalloniatis M, Agrawal R (2020) Normal aging changes in the choroidal angioarchitecture of the macula. Sci Rep 10:10810
20. Breher K, Terry L, Bower T, Wahl S (2020) Choroidal biomarkers: a repeatability and topographical comparison of choroidal thickness and choroidal vascularity index in healthy eyes. Transl Vis Sci Technol 9(11):8
21. Fishman GA, Stone EM, Grover S et al (1999) Variation of clinical expression in patients with Stargardt dystrophy and sequence variations in the ABCR gene. Arch Ophthalmol 117:504–510
22. Sonoda S, Sakamoto T, Yamashita T et al (2015) Luminal and stromal areas of choroid determined by binarization method of optical coherence tomographic images. Am J Ophthalmol 159:1123-1131.e1
23. Sonoda S, Sakamoto T, Yamashita T et al (2014) Choroidal structure in normal eyes and after photodynamic therapy determined by binarization of optical coherence tomographic images. Investig Ophthalmol Vis Sci 55:3893–3898
24. Agrawal R, Wei X, Goud A, Vupparaboina KK, Jana S, Chhablani J (2017) Influence of scanning area on choroidal vascularity index measurement using optical coherence tomography. Acta Ophthalmol 95:e770–e775
25. Battaglia Parodi M, Sacconi R, Romano F, Bandello F (2019) Hyperreflective foci in Stargardt disease: 1-year follow-up. Graefes Arch Clin Exp Ophthalmol 257:41–48
26. Schwoerer J, Secrétan M, Zografos L, Piguet B (2000) Indocyanine green angiography in fundus flavimaculatus. Ophthalmologica 214: 240–245
27. Iovino C, Pellegrini M, Bernabei F et al (2020) Choroidal vascularity index: an in-depth analysis of this novel optical coherence tomography parameter. J Clin Med 9:595
28. Iovino C, Au A, Hilely A et al (2019) Evaluation of the choroid in eyes with retinitis Pigmentosa and cystoid macular edema. Invest Ophthalmol Vis Sci 60:5000–5006
29. Rizzo S, Savastano A, Finocchio L et al (2018) Choroidal vascularity index changes after vitreomacular surgery. Acta Ophthalmol 96:e950–e955
30. Wei X, Mishra C, Kannan NB et al (2019) Choroidal structural analysis and vascularity index in retinal dystrophies. Acta Ophthalmol 97:e116–e121
31. Wei X, Ting DSW, Ng WY, Khandelwal N, Agrawal R, Cheung CMG (2017) Choroidal vascularity index: a novel optical

coherence tomography based parameter in patients with exudative age-related macular degeneration. Retina 37:1120–1125
32. Giannaccare G, Pellegrini M, Sebastiani S et al (2020) Choroidal vascularity index quantification in geographic atrophy using BINARIZATION of enhanced-depth imaging optical coherence tomographic scans. Retina 40:960–965
33. Ratra D, Tan R, Jaishankar D et al (2018) Choroidal structural changes and vascularity index in STARGARDT disease on swept source optical coherence tomography. Retina 38:2395–2400
34. MacHalińska A, Kawa MP, Marlicz W, MacHaliński B (2012) Complement system activation and endothelial dysfunction in patients with age-related macular degeneration (AMD): possible relationship between AMD and atherosclerosis. Acta Opthalmol 90:695–703
35. Nunes RP, Rosa PR, Giani A et al (2015) Choroidal thickness in eyes with central geographic atrophy secondary to stargardt disease and age-related macular degeneration. Ophthalmic Surg Lasers Imaging Retin 46:814–822